

# Gibbs-Sampling-Based Optimization for the Deployment of Small Cells in 3G Heterogeneous Networks

Xiaohang Li\*, Xiaojun Tang<sup>†</sup>, Chih-Chun Wang\*, and Xiaojun Lin\*

<sup>†</sup> AT&T Labs

\* Center for Wireless Systems and Applications, School of ECE, Purdue University

Email: li179@purdue.edu, xt696w@us.att.com, chihw@purdue.edu, linx@ecn.purdue.edu

**Abstract**—The growing popularity of mobile data services has placed great demands for wireless cellular networks to support higher throughput. One way to meet the rapidly growing traffic demand is through heterogeneous network deployment, which uses a mixture of macro cells and small cells (also known as micro- or pico-cells) to further enhance the spatial reuse and thus improves network throughput. In this paper, we propose a Gibbs-sampling based optimization method for the deployment of small cells in 3G networks. To our best knowledge, this work is the first to optimize the locations of multiple small cells with the goal of maximizing a given network utility function. The Gibbs sampling based (GSB) method intelligently balances two potentially conflicting considerations: (i) placing small cells close to congested areas; and (ii) minimizing interference with the existing macro cells and other small cells. We also describe two low-complexity algorithms, the greedy EcNo and the greedy hotspot algorithms. Both algorithms are widely used in industry and will be used as the performance benchmark. Extensive simulations have been conducted based on real traffic traces from the 3G data network. The numerical results show that the GSB placement leads to 10% higher throughput and 30% higher off-loading factor than the greedy solutions.

## I. INTRODUCTION

The proliferation of smartphones and tablets has resulted in much higher data traffic demands on the cellular networks. Between 2007 and 2009 an unprecedented 5000% increase in data traffic has been witnessed [1]. In the USA, nearly 100 million people have subscribed to wireless data plans and used smartphones as one of their main portals for accessing Internet [2]. It is projected that by 2014 an average cell phone user will consume 1GB data per month [3], and the average wireless data connection speed will surpass 1 Mbps in 2014 [4].

To meet the ever-growing demands of higher throughput and better quality-of-service, researchers and providers have considered different ways to expand the network capacity, including the use of multi-antenna techniques, better scheduling and network coding [5]–[7], high-order modulation, and sectorization of the cells. However, these mechanisms are already quite close to their fundamental performance limits, and there is not too much room for further improvement [3]. One promising orthogonal approach is to use small low-power cells (sometimes termed micro/pico base-stations) [8] that complement the regular base stations (sometimes termed the macro base-stations) to further enhance the spatial reuse and improve throughput. Such a cellular network with a mixture

of macro cells<sup>1</sup> and small micro/pico cells [3] is commonly referred to as Heterogeneous Networks (HetNet) (see Fig. 1). The small cells can operate either in the same channel as the macro cells (the co-channel mode), or in different channels than the macro cells (the dedicated small-cell carrier mode). By leveraging the new frequency reuse opportunity, mobile carriers can use the small cells to increase the spectrum efficiency and provide higher network capacity. However, how to deploy the small cells in a HetNet environment is a non-trivial problem. There are two potentially important considerations, i.e., to improve the signal quality and to offload users from macro nodes to small nodes. (We will use the term “small node” and “small-cell base station”, interchangeably.) However, these two objectives could be conflicting. For example, in order to offload more users from macro cells, we would ideally deploy small nodes close to the traffic hotspots<sup>2</sup>. However, small nodes close to each other or close to macro nodes may introduce severe interference, and the signal quality suffers. Thus, the total system throughput may be significantly reduced. Therefore, to optimally place the small nodes, we need to jointly consider both the interference and the traffic demand profile, which is a non-trivial problem.

How to manage interference between macro and pico cells has been studied in LTE networks, and the eICIC (Enhanced Inter-cell Interference Coordination) has been introduced. In contrast, for 3G UMTS/HSDPA, the options of interference management are relatively limited, and hence mainly been studied only in the context of femtocell and femto-user transmission power control [9]. Hence, we believe that in 3G UMTS/HSDPA network, the optimization of small cell placement is even more important in order to control the macro-small cell interference for HetNets.

In the literature, the optimal deployment problem for pico cells have not been extensively studied. [8] has investigated how to use pico cells to improve the performance in UMTS networks under the simple setting of 1 macro node and 1 pico node. [10] studies a similar setting in LTE network, with one macro node and one pico node in the hotspot. In contrast, our work considers the scenario where multiple small nodes will jointly offload the traffic from multiple macro nodes. To our best knowledge, our work is the first to study

<sup>1</sup>The traditional base station in the 3G network is usually termed Node-B. To distinguish from the small nodes, we will use the term “macro node” to refer to the Node-B.

<sup>2</sup>Hotspot indicates an area with high user density.

the small-cell placement problem that jointly optimizes the locations of multiple small nodes with the goal of maximizing a given network utility function. Our work is also related to the femtocell placement problem. Femtocells, as another type of small low-power cells typically deployed indoors, are installed by users instead of cellular operators. They are currently widely employed by cellular carriers, since they can reduce infrastructure and operational expenses (for capacity upgrade) and improve coverage [11]. However, the unplanned deployment and restricted access may cause heavy interference to macro-cell users. The closest solution in the existing literature is the femtocell deployment problem studied in [12]–[14]. However, our work differs significantly from the existing solutions in terms of the objectives and the new consideration of traffic profiles. Specifically, [12], [13] discuss the problem of femtocell placement in a single building. The goal is to minimize the *power consumption for the mobile handsets* while covering “all the service areas in a building.” [14] aims to minimize the *coverage holes* and *pilot transmission power*, which focuses on how to adjust the power control in order to optimize the public coverage space. None of the objectives in [12]–[14] are related in our problem because, in our work the area of interest is already covered by macro nodes. Hence, we do not need to consider coverage as either an objective or a constraint. Further, our work aims to automatically adapt to the traffic demand profiles, which has not been considered in any previous work including [12]–[14].

In this paper, we propose a Gibbs-sampling based optimization method for the deployment of small cells in 3G networks. The Gibbs sampling based (GSB) method intelligently balances the two potentially conflicting considerations discussed earlier: (i) placing small cells close to congested areas; and (ii) minimizing interference with the existing macro cells and other small cells. We also describe two low-complexity algorithms, the greedy EcNo and the greedy hotspot algorithms. Both algorithms are widely used in industry and will be used as the performance benchmark. Extensive simulations have been conducted based on real traffic traces from the 3G data network. The numerical results show that the GSB placement leads to 10% higher throughput and 30% higher off-loading factor than the greedy solutions. In summary, the main contributions of this work are

- We incorporate the traffic demand profiles for different geographical locations into the node placement problem.
- We propose the Gibbs sampling algorithms to optimize the total throughput of all users in the area of interest.
- Empirically, we have conducted extensive simulations based on real traffic traces from existing 3G networks. Our results show that Gibbs sampling converges quickly to the optimal solution and the resulting throughput is 10%-15% better than that of the greedy algorithms.

## II. UMTS/HSDPA HETNET SETTINGS AND MODELS

### A. HetNet Topology and Traffic Profile

We focus on the downlink transmission in a given area adjacent to several macro cells. For ease of exposition, we assume

that the area of interest is rectangular with length  $L$  and width  $W$  (meters). We divide the area into  $N_a \times N_b$  number of rectangular mini-cells. For any mini-cell, the network designer may choose to place a small node (transceiver) in the center of the given mini-cell. Consider the example in Fig 2, for which the area of interest is evenly divided into  $3 \times 3$  mini-cells. We use #1 to #9 to label the 9 mini-cells in Fig. 2, respectively. For the  $k$ -th mini-cell, we use  $c_k$  (Mbps) to represent the data traffic density which is obtained from the statistics of the user activities in the existing network. For example, for the 5-th mini-cell (the center mini-cell), we use #5 : 0.5 to indicate the corresponding data traffic density is 0.5Mbps. Define the normalized traffic density for mini-cell  $j$  as  $\frac{c_j}{\sum_{k=1}^{N_a \times N_b} c_k}$ .

Suppose that there are  $N_m$  macro nodes nearby and our goal is to place  $N_p$  small nodes in the mini-cells. Among the  $N_m + N_p$  transmitters of interest, we use the indices  $n = 1, 2, \dots, N_m$  to denote the existing macro nodes and use the indices  $n = N_m + 1, N_m + 2, \dots, N_m + N_p$  to denote the to-be-placed small nodes. Since any mobile is associated to either a macro node or a small node in HSDPA, we use  $U_n$  to denote the number of users associated with node  $n$  for all  $n = 1, \dots, N_m + N_p$ . For any user  $i$ , we use  $n(i)$  to denote the index of the node with which user  $i$  is associated. We sometimes call  $n(i)$  the serving node of user  $i$ . We use  $U = \sum_{n=1}^{N_m+N_p} U_n$  to denote the total number of users in the area of interest.

### B. HSDPA and Cell Selection

Let  $l_{n,i}$  denote the path loss from cell  $n$  to user  $i$ , for all  $n = 1, \dots, N_m + N_p$  and  $i = 1, \dots, U$ . The path loss denotes the average signal attenuation due to distance-dependent path loss, directional antenna gain, and various fading and shadowing. It can be derived based on network measurements, in which user equipments report the received signal power at their locations. Or, it can be derived based on empirical path loss models after calibration using the data obtained from network measurements and/or drive tests. We assume the power constraint for each small node is  $P_s$  Watt. For the macro nodes, the power constraint may vary and we assume that the power constraint for macro node  $n$  is  $P_m(n)$  Watt. In practice, each node only uses a certain fraction of the max power constraint for data traffic since the node still needs power for supporting voice traffic, control traffic, and broadcast channels



Fig. 1. HetNet is comprised of macro nodes and small nodes. Data traffic on the edge of macro cells are offloaded to the small cells, so that the performance on the macro-cell boundary area is improved and traffic load for the macro cell is alleviated.

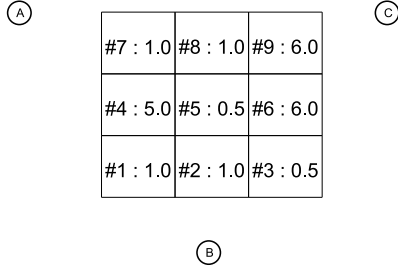


Fig. 2. Illustration of the mini-cells, the corresponding data traffic density, and three coexisting macro nodes.

including CPICH (Common Pilot Channel). The fraction of power available to HSDPA thus varies depending on voice traffic condition and can be estimated by the cellular carrier. We use  $h_f$  to denote the total HSDPA power fraction, i.e., the fraction of power that can be assigned to High Speed Downlink Shared Channel (HS-DSCH). A typical  $h_f$  value is 50% for a macro node and 80% for a small node. Let  $P_n$  (Watt) denote the transmission power of node  $n$ . We assume that even without any data traffic, a node still needs to use  $(1 - h_f)$  of the max power constraint. Therefore, we have for any small node  $n = N_m + 1, \dots, N_m + N_p$ ,

$$P_n = \begin{cases} P_s & \text{if at least 1 user is associated} \\ & \text{with node } n (U_n \geq 1) \\ P_s(1 - h_f) & \text{if } U_n = 0 \end{cases} \quad (1)$$

and for any macro node  $n = 1, \dots, N_m$

$$P_n = \begin{cases} P_m(n) & \text{if } U_n \geq 1 \\ P_m(n) \cdot (1 - h_f) & \text{if } U_n = 0 \end{cases}. \quad (2)$$

The transmission power  $P_n$  and the path loss  $l_{n,i}$  will be used subsequently to compute the SINR and the throughput of individual users.

We now discuss how to compute  $n(i)$ , the serving node of user  $i$ . In HSDPA, each user  $i$  measures CPICH. Then user  $i$  chooses the node that has the largest Received Signal Code Power (RSCP) value (with unit Watt), which is the power level received from the pilot channel of a node. The RSCP value of user  $i$  from a node  $n$  is defined as

$$\text{RSCP}_i^n = \text{Pilot}(n) * l_{n,i}, \quad (3)$$

where  $\text{Pilot}(n)$  (in Watts) denotes the power of the pilot channel for node  $n$ . We assume that for each small node, it uses 10% of its power as the pilot power, i.e.,  $\text{Pilot}(n) = 0.1P_s$  for all  $n = N_m + 1$  to  $N_m + N_p$ . The pilot power for the macro node is from the existing 3G network.

In summary, given the traffic profile  $c_k$  of each individual mini-cell  $k$ , our goal is to find the optimal placement of the  $N_p$  small nodes that maximizes the the throughput of users in the area of interest, based on the long term data traffic geographic information. For the purpose of non-disclosure, we could not explicitly present the data details. Some of the simulation results may only reflect the relative ratios but not

the real values.

### C. HSDPA Throughput Calculation

In this section, we describe an approach to approximate the achievable HSDPA throughput in a static network situation.

The propagation channel from cell node  $k$  to user  $i$  consists of a set of paths, each of which is associated with an average relative received power and delay. Suppose  $l_{k,i}$  is the average path loss from cell  $k$  to user  $i$ . Suppose  $P_{sv}^i$  is the average power that user  $i$  receives from the serving node  $n(i)$ , and  $P_{rv}^i$  is the average total power that user  $i$  receives. Thus, We have

$$P_{sv}^i = P_{n(i)} l_{n(i),i}, \quad (4)$$

$$\text{and } P_{rv}^i = WN_0 + \sum_{k=1}^{N_m+N_p} P_k l_{k,i}, \quad (5)$$

where  $W = 3.84 \times 10^7$  Hz is the WCDMA chip rate and the effective bandwidth of UMTS HSDPA, and  $N_0 = 3.9811 \times 10^{-21}$  watts/Hz is the power spectral density of thermal noise.

For user  $i$ , we use  $\sigma^i$  to denote the ratio of the average total power due to other-cell interference and thermal noise to the average received power from the serving cell, abbreviated as APR. It is calculated by  $\sigma^i = (P_{rv}^i - P_{sv}^i)/P_{sv}^i$ .

A direct calculation of the distribution function of the signal to interference and noise ratio (SINR) is numerically intractable. We followed the method in [15] to estimate the mean and variance as functions of the APR. This approximation is also used by the well-known orthogonality factor model as noted in [15].

We use  $\text{SINR}_i$  to denote the SINR for user  $i$  and  $\text{SINRdb}_i$  to denote the SINR for user  $i$  measured in db, i.e.,  $\text{SINRdb}_i = 10 \log_{10}(\text{SINR}_i)$ . Similar to the four-parametric Weibull functions in [15], we use the following approximation for the mean of  $\text{SINRdb}$  and also the standard deviation  $\text{STD}$  of  $\text{SINRdb}$  in decibel scale.

$$\text{SINRdb}_i = 10 \log_{10}(h_f) + a - be^{-c(\sigma^i)^d}, \quad (6)$$

where  $10 \log_{10}(h_f)$  is the offset in the decibel scale due to the fraction of power available to HSDPA. The empirical parameters  $a, b, c$  and  $d$  are evaluated based on Monte-Carlo numerical simulation for different multi-path profiles defined in 3GPP TS 34.121. The mean and standard deviation allow us to determine the distribution of  $\text{SINRdb}$  under the assumption of a certain distribution model. As shown by the numerical studies in [15], the distribution that achieves the best approximation is the Gaussian distribution (in the decibel scale).

Once  $\text{SINRdb}_i$  is computed, we can compute the Channel Quality Indicator (CQI) according to [16] by

$$\text{CQI}_i = \min(30, \max(0, \lfloor \text{SINRdb}_i/1.02 + 16.62 \rfloor)). \quad (7)$$

Each CQI is an integer number ranging between  $[0, 30]$ . In each Transmit Time Interval (TTI), the Transport Format and Resource Combination (TFRC) selector in HSDPA scheduler decides the number of bits (called Transport Block Size, or TBS) to transmit, based on the CQI value. In 3GPP TS 25.214, TFRCs for different user classes are specified. The

#3 : 0.1	#4 : 0.1
#1 : 0.7	#2 : 0.1

Fig. 3. Example 1 with 4 mini-cells

#3 : 0.3	#4 : 0.3
#1 : 0.1	#2 : 0.3

Fig. 4. Example 2 with 4 mini-cells

CQI-TBS mapping table for a category-10 user is shown in Table I. The average TBS for user  $i$  is given by  $E\{TBS_i\} = \sum_{q=0}^{30} p_i(q)TBS(q)$ , where  $p_i(q)$  is the probability that user  $i$  reports a CQI value  $q$ , and  $TBS(q)$  denotes the TBS value given CQI value  $q$ . (The  $TBS(q)$  value can be derived from Table I.) We assume that HS-DSCH code is not limited, which is the case in real networks. With a round-robin scheduling, the average throughput  $T_{\text{peak}}^i$  for user  $i$  served by cell  $n(i)$  is

$$T_{\text{peak}}^i = \frac{E\{TBS_i\}}{U_{n(i)}(1 + p_e)\text{TTI}}, \quad (8)$$

where  $U_{n(i)}$  is the number of users served by cell  $n(i)$ ,  $\text{TTI} = 2\text{ms}$ ,  $p_e$  is the block error rate, targeted to be 0.1.

#### D. Optimization Objective

We define the  $N_p$ -dimensional position vector

$$\mathbf{s} = (s_{N_m+1}, s_{N_m+2}, \dots, s_{N_m+N_p})$$

to represent the locations of all small nodes. Let  $S$  denote the feasible set, that is, the set of all possible small node placements. We let  $\mathcal{U} : S \rightarrow \mathbb{R}$  to denote the global utility function. In our work, we choose  $\mathcal{U}$  to be the summation of the average throughput for each individual user. However, our solution strategy would work for other types of utility functions of the cell throughput. Note that the actual (average) throughput of user  $i$  has to taking into account time-sharing among all users associated to node  $n(i)$  and is thus computed as  $T_{\text{peak}}^i/U_{n(i)}$ . Our objective function is thus  $\max_{\mathbf{s} \in S} \mathcal{U}(\mathbf{s})$ .

It is clear that the above throughput objective takes into consideration the interference between cells. Further, we argue that the objective of maximizing throughput automatically incorporates the consideration of the data traffic profile. Consider the two 4-mini-cell examples shown in Fig. 3 and 4. Assume

TABLE I  
CQI TO TBS MAPPING FOR CATEGORY-10 USERS (UNIT: NUMBER OF BITS PER BLOCK)

CQI	TBS	CQI	TBS	CQI	TBS
0	0	1	136	2	176
3	232	4	320	5	376
6	464	7	648	8	792
9	928	10	1264	11	1488
12	1744	13	2288	14	2592
15	3328	16	3576	17	4200
18	4672	19	5296	20	5896
21	6568	22	7184	23	9736
24	11432	25	14424	26	15776
27	21768	28	26504	29	32264
30	38576				

that we are deploying one small node in the center of mini-cell 1 in both examples. We also generate  $U$  users for each example according to the respective data traffic profile<sup>3</sup>. Then the total user throughput for Example 1 would be larger than that for Example 2. Specifically, in Example 1, most of the users are in mini-cell 1, and they are closer to the small node. Hence, a larger fraction of users would have a higher peak rate  $T_{\text{peak}}^i$ . Since all users share the bandwidth at a small node  $n(i)$  evenly (i.e., we use  $T_{\text{peak}}^i/U_{n(i)}$  to calculate the actual throughput of such a user), the total throughput of the small node will thus be higher. In contrast, in Example 2, more users are in the surrounding mini-cells, so they are further away from the small node. Then, the throughput would suffer. Thus, by optimizing the total throughput in the area of interest, the solution would tend to deploy small nodes close to the hotspots.

### III. OPTIMIZATION OF SMALL-NODES DEPLOYMENT

Finding the optimal locations for small-cell deployment is highly non-trivial since the complexity of computing the optimal locations grows exponentially  $O((N_a N_b)^{N_p})$  as the number of the to-be-placed nodes increases. In this section, we introduce two low-complexity greedy approaches to deploy the small nodes in the area of interest, which are widely used in industry.

#### A. Greedy EcNo Algorithm

In the first greedy algorithm, the discussions are based on RSCP (see (3)) and EcNo. EcNo is the received energy per chip (Ec) of the pilot channel divided by the total noise power density (No). The following greedy algorithm selects the location based on the EcNo values.

---



---

#### § GREEDY ECNO

- 1: **Input** the traffic profiles, the locations of the macro nodes, and the value of  $U$ , the total number of users.
  - 2: Run the subroutine DECIDE-USER-LOCATIONS.
  - 3: **for**  $n = N_m + 1$  to  $N_m + N_p$  **do**
  - 4: Assume that the locations of all nodes from  $N_m + 1$  to  $n - 1$  have been fixed and there are no small nodes from  $n + 1$  to  $N_m + N_p$ .
  - 5: Temporarily place node  $n$  to the mini-cell  $j$  and calculate the EcNo value for all users and compute the sum of all EcNo:  $\sum_{i=1}^U EcNo(i)$
  - 6: Place node  $n$  to mini-cell  $j^*$  that results in the largest sum of EcNo values for all users.
  - 7: **end for**
  - 8: Associate all users to either the small nodes or the macro nodes according to their RSCP values as discussed in Section II.
- 
- 

The subroutine DECIDE-USER-LOCATIONS is described as follows.

---



---

#### § DECIDE-USER-LOCATIONS

<sup>3</sup>The user generation part can be carried out by the subroutine DECIDE-USER-LOCATIONS discussed in Section III-A.

- 1: For each user, it has probability  $\frac{c_j}{\sum_{k=1}^{N_a \times N_b} c_k}$  to be assigned to mini-cell  $j$ .
- 2: For each user that is assigned to mini-cell  $j$ , uniformly generate a position within mini-cell  $j$ .
- 3: The location of each user will be used to compute the average path loss  $l_{n,i}$  for the subsequent computations.

### B. Greedy Hotspot Algorithm

To best offload traffic from the macro cells, it is intuitive to deploy small nodes in the vicinity of the traffic hotspots, which inspires the following even simpler, location-based greedy algorithm that does not involve the computation of the path losses, etc.

#### § GREEDY HOTSPOT

- 1: **Input** the traffic profiles.
- 2: **for**  $n = N_m + 1$  to  $N_m + N_p$  **do**
- 3: Among all the mini-cells which do not have any small node deployed, choose the one with the highest data traffic volume (see Fig. 2) and place node  $n$  in that mini-cell.
- 4: **end for**

### C. Discussion

Both greedy EcNo and greedy hotspot algorithms have low complexity. However, their performances could be highly suboptimal. Take the traffic profile in Fig. 2 for example. Suppose that we would like to deploy two small nodes. Apparently, greedy hotspot algorithm would choose mini-cell 9 and mini-cell 6 since they have the largest data traffic density (both being 6). However, it is likely that the users close to mini-cells 1, 4, and 7 will not be offloaded according to such node placement. For the greedy EcNo algorithm, it is likely that it will choose mini-cell 5 first, since placing a small node right in the center can result into the maximum sum of the EcNo values. After placing the first node in mini-cell 5, the greedy algorithm will chose mini-cell 9 for the second small node as it has the highest traffic density among all peripheral mini cells. On the other hand, one can quickly see that a better deployment would be to choose mini-cells 4 and 6, which covers two of the highest density regions while the small nodes being separated far enough to reduce co-channel interference. This example illustrates the importance of jointly optimizing all small node locations simultaneously when compared to the greedy solutions.

## IV. GIBBS SAMPLING FOR OPTIMIZATION OF SMALL NODE LOCATION

We next propose an optimization algorithm based on Gibbs sampling. Our goal is to optimize the small nodes locations so that the total utility for the users in the area of interest can be improved. The basic idea is as follows. First we place all small nodes randomly: each small node randomly chooses one mini-cell. Then, in each iteration, each small

node one-by-one decides (for itself) whether to relocate to to a neighboring mini-cell according to a probability distribution and re-associate with users. Based on the above construction, the locations of the small nodes form a stochastic process. By carefully choosing the probability whether a small node should change location, we can ensure that the steady state distribution of the stochastic process is concentrated (in some sense of probability) around the global optimal solution.

Recall that the  $N_p$ -dimensional position vector

$$\mathbf{s} = (s_{N_m+1}, s_{N_m+2}, \dots, s_{N_m+N_p})$$

represents the locations of all small nodes. We use  $\mathbf{s}_{\setminus n}$  to represent the  $N_p-1$  small-node locations except the small node  $n$ , and  $(\mathbf{s}_{\setminus n}, b_n)$  to denote the  $N_p$ -dimensional vector

$$(s_{N_m+1}, \dots, s_{n-1}, b_n, s_{n+1}, \dots, s_{N_m+N_p}),$$

which replaces  $s_n$ , the location of small node  $n$ , by  $b_n$ . Recall that  $S$  denotes the feasible set. Let  $S^* \subseteq S$  be the set of optimal solutions that maximize the global utility function  $\mathcal{U} : S \rightarrow \mathbb{R}$ . Recall that in our work, we choose  $\mathcal{U}$  to be the summation of the average throughput for each individual user.

For discussion, we use  $t$  to denote the number of Gibbs sampling iterations. The goal is to design the transition probability such that the steady-state distribution ( $t \rightarrow \infty$ ) is

$$\pi(\mathbf{s}) = \frac{e^{\gamma \mathcal{U}(\mathbf{s})}}{\sum_{\mathbf{s}' \in S} e^{\gamma \mathcal{U}(\mathbf{s}')}}, \quad (9)$$

where  $\gamma > 0$  is a fixed parameter. This distribution is called the Gibbs measure [17]. When  $\gamma$  is large, the steady-state distribution being (9) means that with high probability, the steady-state will concentrate on the optimal solution  $\mathbf{s}^*$  (the one that has the largest  $\mathcal{U}(\mathbf{s})$  value). The *Gibbs sampler* to be presented below drives the small node placement Markov chain to the steady state distribution (9).

For each iteration (we assume that within each iteration we update the node location sequentially from node  $n = N_m + 1$  to  $N_m + N_p$ ). Let the current small node placement be  $\mathbf{s} \in S$  and assume small node  $n$  is updating its location. Node  $n$  can jump up, down, left, right by one mini-cell, or remain in the original mini-cell. We again use Fig. 2 for example. Suppose that small node  $n$  originally locates in mini-cell 5. In one update process, it can choose to move to mini-cell 8, mini-cell 2, mini-cell 4, or mini-cell 6. Or, it can simply remain in mini-cell 5. For the small node on the boundary of the area of interest, it can jump around the boundary. For example, mini-cell 9 can move to mini-cell 3, mini-cell 6, mini-cell 8, or mini-cell 7. Or, it can stay in mini-cell 9. Let  $P(b_n | \mathbf{s})$  be the probability that small node  $n$  updates its location to  $b_n$ . According to the current location of node  $n$ , each node has 5 possible new locations  $b_n$ . The Gibbs sampler in [17] set the transition probabilities as

$$P(b_n | \mathbf{s}) = \frac{e^{\gamma \mathcal{U}(b_n, \mathbf{s}_{\setminus n})}}{\sum_{\forall \text{valid new locations } b'_n} e^{\gamma \mathcal{U}(b'_n, \mathbf{s}_{\setminus n})}}. \quad (10)$$

The detailed Gibbs sampling algorithm is described as follows.

---



---

## § GIBBS SAMPLING

- 1: **Input** The traffic profiles, the locations of the macro nodes, and the value of  $U$ , the total number of users.
  - 2: Run the subroutine DECIDE-USER-LOCATIONS.
  - 3: **for**  $t = 1$  to **max-iter**, the maximum number of allowed iterations **do**
  - 4:   **for** each small node  $n$  **do**
  - 5:     Tentatively move the small node up, down, left, right by one mini-cell, or remain in the original mini-cell
  - 6:     Calculate throughput for each user and compute the sum of all throughputs.
  - 7:     Using the 5 computed summations of throughput (corresponding to different transitions respectively) to calculate transition probability according to (10).
  - 8:     Using the distribution (10), randomly choose the mini-cell that the small node  $n$  will jump to.
  - 9:     Update the node association for each user.
  - 10:   **end for**
  - 11: **end for**
- 
- 

We now have the following lemma that quantifies the performance of the above Gibbs sampler.

**Lemma 1.** *When  $t \rightarrow \infty$ , the difference between the global optimal utility  $U(s^*)$  and the expected utility generated by the Gibbs sampler in (10) no larger than  $\frac{1}{\gamma} \log(\frac{|S|}{|S^*|})$ .*

*Proof:* Considering any optimal solution  $\mathbf{s}^* \in S^*$ , we have

$$\begin{aligned} \mathbb{E}\{e^{\gamma(\mathcal{U}(\mathbf{s}^*) - \mathcal{U}(\mathbf{s}))}\} &= \sum_{\mathbf{s} \in S} e^{\gamma(\mathcal{U}(\mathbf{s}^*) - \mathcal{U}(\mathbf{s}))} \pi(\mathbf{s}) \\ &= \sum_{\mathbf{s} \in S} \frac{\pi(\mathbf{s}^*)}{\pi(\mathbf{s})} \pi(\mathbf{s}) = |S| \pi(\mathbf{s}^*) \leq \frac{|S|}{|S^*|}, \end{aligned} \quad (11)$$

where the last step is because  $\pi(\mathbf{s}^*) \leq \frac{1}{|S^*|}$ . By Jensen's inequality, we have

$$e^{\gamma(\mathcal{U}(\mathbf{s}^*) - \mathbb{E}\{\mathcal{U}(\mathbf{s})\})} \leq \mathbb{E}\{e^{\gamma(\mathcal{U}(\mathbf{s}^*) - \mathcal{U}(\mathbf{s}))}\} \leq \frac{|S|}{|S^*|}. \quad (12)$$

By taking logarithm on both sides, we have

$$\mathbb{E}\{\mathcal{U}(\mathbf{s})\} \geq \mathcal{U}(\mathbf{s}^*) - \frac{1}{\gamma} \log\left(\frac{|S|}{|S^*|}\right). \quad (13)$$

■

The implication of Lemma 1 is that, as  $\gamma \rightarrow \infty$ , the expected utility generated by the Gibbs sampler approaches the optimal value. The cost of using larger  $\gamma$  is the convergence speed. For practical settings we can choose a  $\gamma$  that strikes proper tradeoff between optimality and the convergence speed.

## V. SIMULATION

In our simulation, all the configurations about the macro nodes are from an existing 3G network. We assume that each small node's height is 3.5 meter and each user equipment's height is 0.75 meter. Let  $d_{n,i}$  denote the Euclidean distance

between user  $i$  and cell  $n$ . We assume that each small node is omnidirectional, and the path loss between small node  $n$  and user  $i$  is given by

$$l_{n,i} = -30.7 - 38 \times \log_{10}(d_{n,i}) \quad (\text{unit: decibel}). \quad (14)$$

For macro node  $n$ , the model for deciding the average path losses can be found in [18], [19]. In our simulation, the multipath profile we consider is ITU Pedestrian A. Similar to [15], we run Monte Carlo simulations to obtain the parameters in (6), where we set  $a = 9.23$ ,  $b = 55.78$ ,  $c = 1.62$ , and  $d = -0.22$ .

We run simulations over 3 data sets from an existing 3G network in a metropolitan area on the US western coast. Due to space constraints, we only show in details the results for data set 1 and list the results for data sets 2 and 3 in [20]. For data set 1, the area of interest has length  $L = 700$  meters and width  $W = 700$  meters. We evenly divide this area into 49 mini-cells. Thus, each mini-cell is exactly 100 meters long and 100 meters wide. In the area of interest, the data traffic density for each mini-cell is also obtained from the existing 3G network. In Fig. 5, we show the relative data density value by a heat map.

### A. Performance Comparison

We compare the performance of Gibbs sampling, greedy EcNo, and greedy hotspot in terms of the average throughput<sup>4</sup> per user, the average throughput per cell, and the offloading factor. Among them, the offloading factor is defined as the ratio of the number of users who have been offloaded from macro nodes to small nodes, over the total number of all users in the area of interest. As we have explained in Section I, the offloading factor is important because as more users are offloaded, the burden on the macro nodes will be lower. Thus, the throughput and dropping rate for macro nodes can also be enhanced.

We divide the simulation into two stages: design and evaluation. In the design stage, we run different schemes in order to find a deployment decision for the small nodes. Then, in the evaluation stage, we fix the node placement of each scheme and run Monte Carlo simulations to measure the average cell/user throughput, and the offloading factor so that we can compare the relative performance.

In the design stage, for the greedy EcNo and for the Gibbs sampling schemes, we choose the total number of users<sup>5</sup> being 4900. Then, we run the Gibbs sampling, greedy EcNo, and greedy hotspot algorithms respectively, to obtain the deployment locations for all small nodes.

In the real world, it is unlikely that there are as many as 4900 simultaneous users in the area of interest. However, when there are only a small number of users, the randomness of the user locations will lead to different throughput even after we have fixed the small node locations after the design stage. Thus, in the evaluation stage we run the simulation with only

<sup>4</sup>We assume all the throughput in the simulation is counted as Mbps.

<sup>5</sup>A large number of users help to capture the traffic demand information.

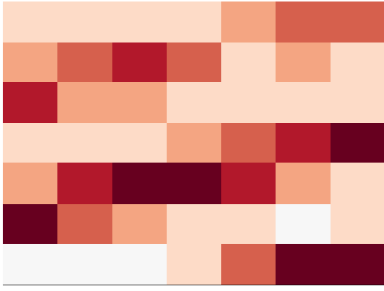


Fig. 5. Illustration relative data traffic density in  $7 \times 7$  mini-cells. The darker the color in each mini-cell is, the heavier the traffic density is.

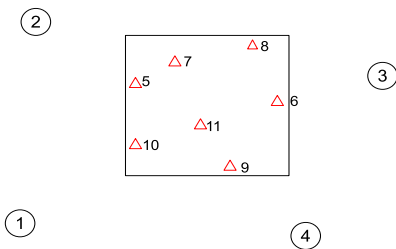


Fig. 6. Map for the area of interest with small nodes (red triangle) and macro nodes (black circle)

10 users and calculate the corresponding throughput and the offloading factor. By repeating the 10-user simulation for 1000 times, we measure the average throughput and the offloading factor.

Fig. 6 shows the geographical information of data set 1. The circles represent the 4 macro nodes. As we can see, the area of interest (a square) is far away from the 4 macro nodes and is on the boundary of the macro cells. The red markers inside the square represent locations of the small nodes produced by Gibbs sampling algorithm and the numbers represent the node index. Fig. 7, 8, and 9 show the fixed locations of the small nodes. We can also show the randomly generated users together with the placement of small nodes. Due to the space limit, we put the details in our technical report [20].

Due to the space constraints, we only discuss the deployment with 7 small nodes in the area of interest. In Figs. 7, 8, and 9, we show the deployment designs for greedy EcNo, greedy hotspot, and Gibbs sampling algorithms. In Fig. 7, the greedy EcNo algorithm first places small node 5 in the center of the area, in order to greedily maximize the total EcNo value of all users. All other nodes are deployed likewise. In Fig. 8, the greedy hotspot algorithm places all the small nodes on the hotspots, while ignoring all the mini-cells on the upper side of the map. In contrast, the Gibbs sampling approach jointly considers the user signal quality and geographic traffic information, and results in the decision in Fig. 9. In this deployment, near every hotspot we can find a small node, and all small nodes are spreaded out so that the interference is lower.

In Fig. 10, we show the cumulative distribution function of

the summation of the throughput for 1000 instances of Monte Carlo simulation and each instance has 10 users. We can see the median throughput improvement of the Gibbs sampling versus greedy is 16% percent and can be as large as 0.25 Mbps. The average per-user throughputs are 1.63, 1.43, and 1.41 Mbps for the three schemes respectively and we also see 15% improvement to the greedy EcNo solution. Fig. 11 studies the benefits of Gibbs sampling versus the number of small nodes to be placed. As can be seen that with 7 small nodes, HetNet with Gibbs sampling offers 5 times the throughput of the original network. When compared to the greedy approaches, Gibbs sampling also offers 10% throughput improvement, which is quite substantial considering the actual cost of the node placement. Further, the throughput gap between Gibbs sampling and the greedy approach becomes larger when considering more small nodes, which is due to the fact that Gibbs sampling jointly optimizes all the locations while the greedy solution takes a myopic approach.

Fig. 12 studies the benefits in terms of offloading factors. We see that with 7 small nodes Gibbs sampling successfully offloaded on almost all users to the small nodes. The offloading for greedy solutions are patchy since it places one node at a time and does not coordinate the placements of all small nodes. We also show that the Gibbs sampling approach can get stable after 15 iterations. Due to the space limit, the details can be found in [20].

## VI. CONCLUSION

In this paper, we study the optimization for deployment of small nodes in a 3G HetNet environment. To our best knowledge, this work is the first solution for the placement of small-cell base-stations that jointly optimizes the locations of multiple small nodes with the goal of maximizing any given network utility function. We first present a couple of low-complexity greedy algorithms for which the performance can be unsatisfactory. We then propose to use Gibbs sampling to optimize the small node deployments. The Gibbs Sampling method intelligently balances two potentially conflicting considerations: (i) placing small-cell BSs close to high-traffic areas; and (ii) avoiding co-channel interference with the macro-cell BSs and other small cell BSs. We show that the Gibbs sampling can be made very close to optimal. Simulation results based on the data set from an existing 3G network show that Gibbs sampling can consistently lead to better throughput and better offloading factors when compared to the greedy algorithms.

For future work, we plan to take into account additional interference management mechanisms. For example, neighbor cells can further schedule their transmission in the time domain and/or adjust their transmission power to avoid co-channel interference. It would be interesting to see what the deployment decisions should be when further taking into account the optimal scheduling and power control mechanisms.

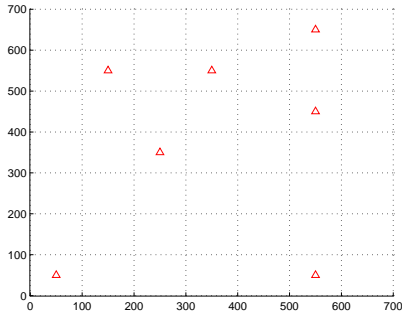


Fig. 7. Deployment map for greedy EcNo algorithm with 7 small nodes

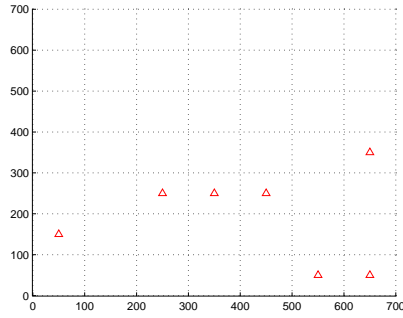


Fig. 8. Deployment map for greedy hotspot algorithm with 7 small nodes

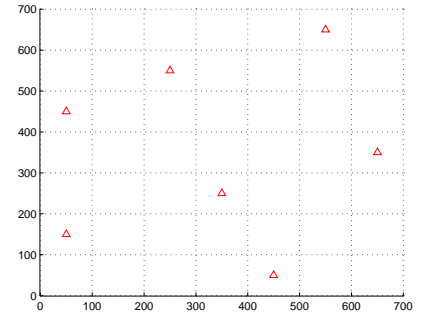


Fig. 9. Deployment map for Gibbs sampling algorithm with 7 small nodes

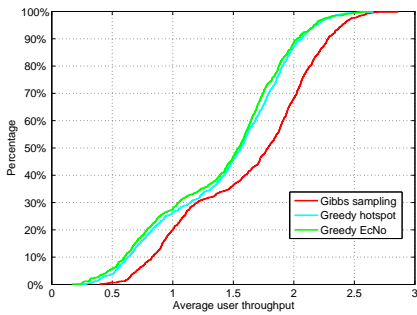


Fig. 10. CDF for Gibbs sampling, greedy EcNo, and greedy hotspot in 1000 instances of Monte Carlo simulation of evaluation stage

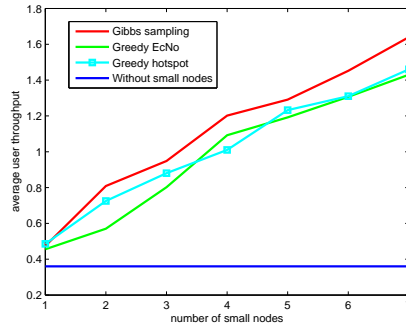


Fig. 11. The average user throughput with different number of small nodes

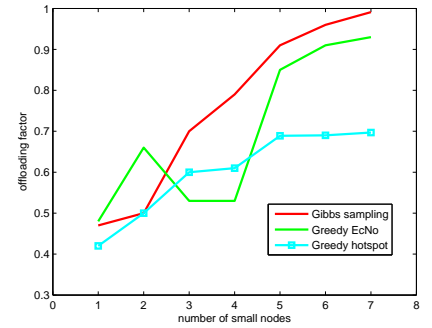


Fig. 12. The offloading factor with different number of small nodes

## VII. ACKNOWLEDGEMENT

This work has been partially supported by the NSF grants CNS-0721484, CNS-0721477, CNS-0643145, CCF-0845968, CNS-0905331, and a grant from Purdue Research Foundation.

## REFERENCES

- [1] M. Meeker, S. Devitt, and L. Wu, "Economy + internet trends," in *Web 2.0 Summit*. Morgan Stanley Research, 2009.
- [2] "2012 mobile future in focus," *comScore*, 2012.
- [3] S. Landström, A. Furuskär, K. Johansson, L. Falconetti, and F. Kronstedt, "Heterogeneous networks—increasing cellular capacity," *The data boom: opportunities and challenges*, 2011.
- [4] "Cisco visual networking index: Global mobile data traffic forecast update, 2011-2016."
- [5] X. Li, C.-C. Wang, and X. Lin, "Throughput and delay analysis on uncoded and coded wireless broadcast with hard deadline constraints," in *Proc. of INFOCOM, mini conference*, 2010.
- [6] —, "On the capacity of immediately-decodable coding schemes for wireless stored-video broadcast with hard deadline constraints," *IEEE J. Sel. Areas Commun.*, vol. 29, no. 5, pp. 1094–1105, May 2011.
- [7] —, "Optimal immediately-decodable inter-session network coding (idnc) schemes for two unicast sessions with hard deadline constraints," in *Proc. of Allerton Conference, invited paper*, 2011.
- [8] D. Pouhe, D. Emini, and M. Salbaum, "The use of microcells as a means of optimizing umts networks," in *Proc. of WFMN*, 2007.
- [9] M. Yavuz, F. Meshkati, S. Nanda, A. Pokhariyal, N. Johnson, B. Raghathan, and A. Richardson, "Interference management and performance analysis of umts/hspa+ femtocells," *IEEE Commun. Mag.*, vol. 47, no. 9, pp. 102–109, 2009.
- [10] S. Landstrom, H. Murai, and A. Simonsson, "Deployment aspects of lte pico nodes," in *Proc. of ICC*, 2011.
- [11] V. Chandrasekhar, J. Andrews, and A. Gatherer, "Femtocell networks: a survey," *IEEE Commun. Mag.*, vol. 46, no. 9, pp. 59–67, 2008.
- [12] J. Liu, T. Kou, Q. Chen, and H. Sherali, "Femtocell base station deployment in commercial buildings: A global optimization approach," *IEEE J. Sel. Areas Commun.*, vol. 30, no. 3, pp. 652–663, 2012.
- [13] J. Liu, Q. Chen, and H. D. Sherali, "Algorithm design for femtocell base station placement in commercial building environments," in *Proc. of INFOCOM*, 2012.
- [14] I. Ashraf, H. Claussen, and L. T. W. Ho, "Distributed radio coverage optimization in enterprise femtocell networks," in *Proc. of ICC*, 2010.
- [15] D. Staehle and A. Mader, "A model for time-efficient hsdpa simulations," in *VTC 2007*.
- [16] F. Brouwer, I. de Bruin, J. Silva, N. Souto, F. Cercas, and A. Correia, "Usage of link-level performance indicators for hsdpa network-level simulations in e-umts," in *ISSSTA 2004*.
- [17] P. Brémaud, *Markov chains: Gibbs fields, Monte Carlo simulation, and queues*. Springer, 1999, vol. 31.
- [18] "3gpp standards," *TR 36.814*, 2010.
- [19] F. Gunnarsson, M. Johansson, A. Furuskär, M. Lundevall, A. Simonsson, C. Tildestav, and M. Blomgren, "Downtilted base station antennas—a simulation model proposal and impact on hspa and lte performance," in *VTC 2008*.
- [20] X. Li, X. Tang, C.-C. Wang, and X. Lin, "Gibbs-sampling-based optimization for the deployment of small cells in 3g heterogeneous networks," *Technical Report, Purdue University*, <http://docs.lib.purdue.edu/ecetr/440/>, 2013.